Published on 26 November 2009. Downloaded by State University of New York at Stony Brook on 23/10/2014 19:43:42.

This article is published as part of the *Dalton Transactions* themed issue entitled:

New Talent

Showcasing the strength of research being carried out by tomorrow's leaders in the field of inorganic chemistry

Guest Editor Polly Arnold
University of Edinburgh, UK

Published in issue 2, 2010 of *Dalton Transactions*

Image reproduced with permission of Mark Muldoon

Articles in the issue include:

PERSPECTIVES:

Modern multiphase catalysis: new developments in the separation of homogeneous catalysts
Mark J. Muldoon, *Dalton Trans.,* 2010, DOI**:** 10.1039/b916861n

Probing bioinorganic chemistry processes in the bloodstream to gain new insights into the origin of human diseases
Elham Zeini Jahromi and Jürgen Gailer, *Dalton Trans.,* 2010, DOI: 10.1039/b912941n

COMMUNICATIONS:

Facile entry to 3d late transition metal boryl complexes
Ba L. Tran, Debashis Adhikari, Hongjun Fan, Maren Pink and Daniel J. Mindiola**,**
Dalton Trans., 2010, DOI: 10.1039/b912040h

Probing the kinetics of ligand exchange on colloidal gold nanoparticles by surface-enhanced raman scattering
Yuhua Feng, Shuangxi Xing, Jun Xu, Hong Wang, Jun Wei Lim and Hongyu Chen,
Dalton Trans., 2010, DOI: 10.1039/b912317b

Visit the *Dalton Transactions* website for more cutting-edge inorganic and organometallic research
www.rsc.org/dalton

Published on 26 November 2009. Downloaded by State University of New York at Stony Brook on 23/10/2014 19:43:42.

Acetylenedithiolate as directional bridging ligand in cobalt(I) alkyne platinum dithiolato bimetallic complexes†

Wolfram W. Seidel,*[a,b] Matthias J. Meel,[b] Florian Hupka[b] and Jan J. Weigand[b]

Received 15th July 2009, Accepted 18th November 2009
First published as an Advance Article on the web 26th November 2009
DOI: 10.1039/b913859e

The η²-*C*,*C*′-acetylenedithiolate (acdt^{2-}) complex K[(triphos)Co(acdt)], K-**5**, {triphos = 1,1,1-tris(diphenylphosphinomethyl)ethane} was obtained by consecutive removal of *S*-protection groups in [(triphos)Co(**1**)]PF$_6$, **3**-PF$_6$ (**1** = 1-Trimethylsilyl-7-phenyl-3,6-dithiahept-4-ine). Reaction of K-**5** with selected Pt(II) salts resulted in the formation of the new heterobimetallic complexes [(phen)Pt(**5**)]BPh$_4$, **6**-BPh$_4$, (phen = 1,10-phenanthroline) and [(dppe)Pt(**5**)]BPh$_4$, **7**-BPh$_4$, {dppe = 1,2-bis(diphenylphosphino)ethane}, which were fully characterized. X-ray diffraction studies showed that Co and Pt are linked by acdt^{2-} in the η²-*C*,*C*′-κ²-*S*,*S*′-bridging mode. The electronic structure of **6**-BPh$_4$ and **7**-BPh$_4$ was investigated by electronic absorption spectroscopy, cyclic voltammetry and X-band EPR spectroscopy of neutral **7**. In addition, NMR spectroscopy, X-ray diffraction and reactivity studies with the alkyne complexes [(PMe$_3$)$_3$Co(**1**)]-PF$_6$, **2**-PF$_6$, with **3**-PF$_6$ and the intermediate product [(triphos)Co{η²-(S)C$_2$(SCH$_2$Ph)}], **4**, uncovered the flexibility of the CoC$_2$S$_2$-moiety within the persisting complex scaffold throughout the synthetic scheme.

Introduction

Heteropolymetallic complexes with strong electronic ligand mediated cooperation of the metal centers receive continuing attention due to their often attractive photophysical or magnetic behavior. Functional materials with useful magnetic properties are frequently constructed by the assembly of mononuclear complexes by small bridging ligands like cyanide.[1-4] In addition, fundamental catalytic processes caused by light driven charge separation are generally based on ligand mediated metal–metal interaction and bimetallic reaction patterns.[5-7]

In this respect we are devoted to the coordination chemistry of acetylenedithiolate (acdt^{2-}), (S–C≡C–S)$^{2-}$, which is furnished with donor ability at each atom of the ligand. The coordination chemistry of related alkyne-1-thiolates and recently emerged[8] highly attractive diynedithiolates (S–C≡C–C≡C–S)$^{2-}$ is dominated by the thiolato group[9-13] and examples exhibiting both η²-alkyne- and thiolato-coordination are rare.[14,15] Nonetheless, the combination of both alternatives, side on alkyne binding and dithiolato chelate coordination, confer to the doubly charged acdt^{2-} directionality. Provided that two different donor atoms are present, this type of bridging metals is the shortest possible and is related to the ubiquitary cyanide ion. However, in addition to the short path between the metals acdt^{2-} exerts a chelate effect of the dithiolene type.

In our ongoing studies we have demonstrated that the bend-back angle in η²-*C*,*C*′-alkyne complexes of acdt^{2-} is flexible enough to allow for the κ²-*S*,*S*′-chelate coordination to a second metal ion.[16-18] Bi- and trimetallic complexes with acdt^{2-} in this η²-*C*,*C*′-κ²-*S*,*S*′-bridging mode display redox-variability and visible transitions with high absorptivity. Particularly, investigations on [{Tp′W(CO)$_2$(acdt)}$_2$M] {M = Ni, Pd, Pt; Tp′ = Hydrotris(3,5-dimethylpyrazolyl)borate; Fig. 1} indicated strong electronic coupling of metals over acdt^{2-}-bridges. However, preparative access to complexes of this type is hampered by the fact that the free acetylenedithiol is intrinsically unstable.[19-21] Therefore, the synthetic strategy comprises formation of alkyne complexes with appropriate acetylenedisulfides and subsequent generation of alkyne complexes of acdt^{2-} in the complex. This procedure requires well adapted sulfur-protection groups and respective deprotection conditions in order to retain the alkyne complex moiety. Anionic complexes of the type [Tp′M(CO)(L)(acdt)]$^-$ (M = Mo, W; L = CO, RNC) were obtained by reductive removal of benzyl groups in the corresponding cationic bis(benzylthio)acetylene complexes.[22] Attempts to expand the type of metal bound to carbon from Mo/W(II) to Co(I) revealed the need for a milder procedure implying nucleophilic removal of trimethylsilylethyl *S*-protection groups.

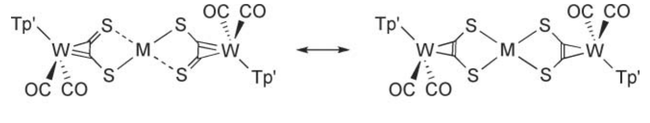

M = Ni, Pd, Pt

Fig. 1 Mesomeric forms of trinuclear complexes linked by acdt^{2-}.

Alkyne complexes of Co(I) are prone to C–C-coupling reactions of coordinated alkynes.[23,24] This applies particularly to the [(η⁵-C$_5$H$_5$)Co] moiety,[25] but it has also been observed at [(PMe$_3$)$_3$Co].[26,27] In order to suppress this reactivity we have chosen

---

[a] *Institut für Chemie, Universität Rostock, Albert-Einstein-Straße 3a, 18059, Rostock, Germany. E-mail: wolfram.seidel@uni-rostock.de; Fax: +49 (0)381 4986382; Tel: +49 (0)381 4986380*

[b] *Institut für Anorganische und Analytische Chemie, Westfälische Wilhelms-Universität Münster, Corrensstraße 30, 48149, Münster, Germany*

† Electronic supplementary information (ESI) available: Additional spectroscopic data, EPR measurement and simulation details. CCDC reference numbers 740232–740236. For ESI and crystallographic data in CIF or other electronic format see DOI: 10.1039/b913859e

Published on 26 November 2009. Downloaded by State University of New York at Stony Brook on 23/10/2014 19:43:42.

1,1,1-tris(diphenylphosphinomethyl)ethane (triphos) as ancillary ligand. The ability of the [(triphos)Co(I)] unit to form stable alkyne complexes has already been shown.[28]

In this contribution we describe the generation of a novel η^2-*C*,*C′*-alkyne complex of acdt^{2-} with the [(triphos)Co(I)] moiety and the subsequent formation of heterobimetallic complexes with the building blocks [Pt(phen)]$^{2+}$ and [Pt(dppe)]$^{2+}$ {phen = 1,10-phenanthroline, dppe = 1,2-bis(diphenylphosphino)ethane}. The molecular structures, the spectroscopic properties and finally the electronic structures of the bimetallic complexes are discussed.

Results and discussion

Mononuclear alkyne complexes

Alkyne complexes of acetylenedisulfides with [(PMe$_3$)$_3$Co(I)] are easily accessible by the method of *Dartiguenave*[26] by reaction of [(PMe$_3$)$_3$Co(Br)] with the appropriate alkyne in acetonitrile and subsequent addition of an alkali metal salt. This procedure can also be used for [(triphos)Co(I)] with the tripodal triphosphine. A competing coordination of the sulfide group was not observed. Using the unsymmetrically substituted alkyne **1** (Scheme 1), which was synthesized from Me$_3$SiCCH in a stepwise manner, the spectroscopically pure complexes [(PMe$_3$)$_3$Co(**1**)](PF$_6$), **2**-PF$_6$, and [(triphos)Co(**1**)](PF$_6$), **3**-PF$_6$, were obtained after addition of KPF$_6$ and chromatographic purification of the crude products. Both complexes are air-stable and crystallization of **2**-PF$_6$ from CH$_2$Cl$_2$–n-hexane solution or slow evaporation of the solvent from a solution of **3**-PF$_6$ in methanol yielded crystals suitable for X-ray diffraction. The molecular structures are shown in Fig. 2 and selected interatomic distances and angles are listed in Table 1.

Table 1 Selected distances (Å) and angles (°) for **2**$^+$, **3**$^+$ and **4**

	2$^+$	**3**$^+$	**4A**[a]	**4B**[a]
Co–C1	1.836(2)	1.844(5)	1.876(3)	1.865(4)
Co–C2	1.862(2)	1.848(5)	1.821(3)	1.821(3)
C1–C2	1.320(2)	1.342(7)	1.346(5)	1.343(5)
C1–S1	1.703(2)	1.695(5)	1.665(3)	1.669(4)
C2–S2	1.702(2)	1.706(5)	1.691(3)	1.691(3)
Co–P1	2.169(1)	2.221(2)	2.186(1)	2.182(1)
Co–P2	2.220(1)	2.155(2)	2.154(1)	2.151(1)
Co–P3	2.147(1)	2.220(2)	2.193(1)	2.196(1)
C1–C2–S2	148.1(2)	129.8(4)	140.1(3)	140.0(3)
C2–C1–S1	148.9(2)	141.4(4)	142.7(3)	143.1(3)

[a] A and B represent the two individual molecules in the asymmetric unit.

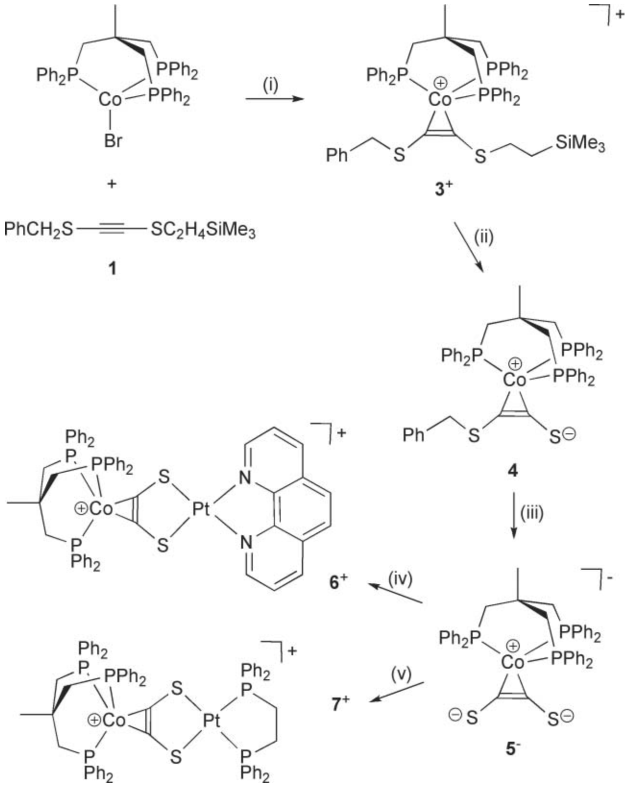

Scheme 1 Complex synthesis: (i) KPF$_6$, CH$_3$CN; (ii) Bu$_4$NF, thf; (iii) C$_8$K, thf; (iv) [PtCl$_2$(phen)], NaBPh$_4$, thf; (v) [PtCl$_2$(dppe)], NaBPh$_4$, thf.

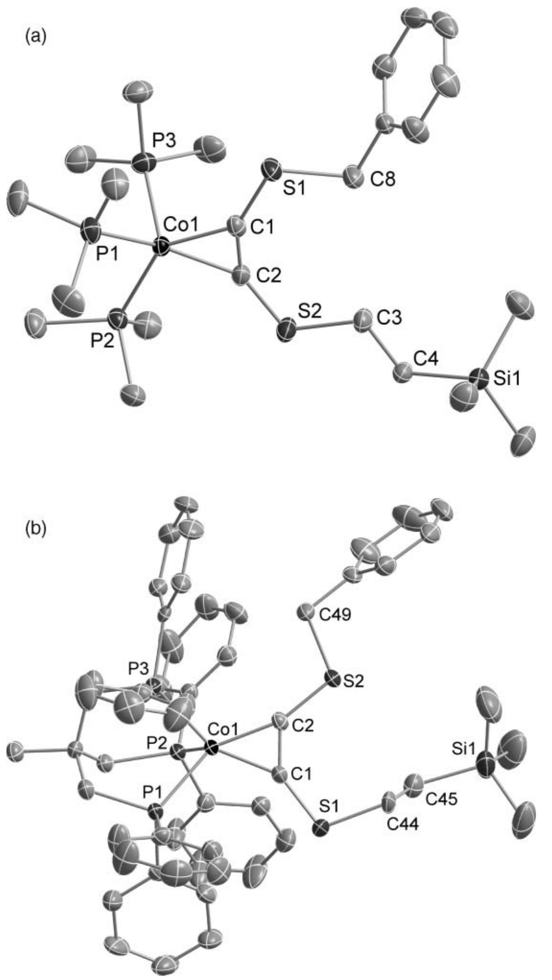

Fig. 2 Molecular structures of cations **2**$^+$ (a) and **3**$^+$ (b) showing 50% probability ellipsoids and atom labelling scheme. Hydrogen atoms and counter ions are omitted for clarity.

The molecular structure of both complex cations shows a distorted tetrahedral geometry considering the alkyne as occupying a single coordination site. The variations in the CoC$_2$ unit between **2**$^+$ and **3**$^+$ are marginal. Considering the more tied position of the phosphorus atoms at the Co center and the weaker donor strength of the diarylphosphine group in **3**$^+$ this

Published on 26 November 2009. Downloaded by State University of New York at Stony Brook on 23/10/2014 19:43:42.

observation is surprising. Thus, the P–Co–P angles in **2**$^+$ fall around an average of 100.0°, whereas in **3**$^+$ with the chelating triphos ligand the mean P–Co–P angle amounts to 90.3°. A significant difference between complexes of sulfur-substituted and carbon based alkynes is the C_{sp}–C_{sp} distance being smaller in the latter case. The C1–C2 bond lengths amount to 1.320(3) Å in **2**$^+$ and 1.342(7) Å in **3**$^+$, while the corresponding values are 1.265(7) Å in [(PMe$_3$)$_3$Co(PhC≡CPh)]$^+$ and 1.264(8) Å in [(PMe$_3$)$_3$Co(PhC≡CC$_5$H$_{11}$)]$^+$.[26,27] The only other structurally characterized alkyne complex with the [(triphos)Co]$^+$ unit, [(triphos)Co(^{t}BuC≡C–C≡C^{t}Bu)]$^+$, displays a C_{sp}–C_{sp} bond of 1.313(8) Å.[28] This medium value is an indication that the longest C_{sp}–C_{sp} bond in **3**$^+$ is due to both sulfur substitution and the triphos ancillary ligand.

A striking difference between **2**$^+$ and **3**$^+$ applies to the bend-back angles of the sulfur substituents. In **2**$^+$ the C_{sp}–C_{sp}–S angles are both larger than 148°, while one of the corresponding angles in **3**$^+$, C1–C2–S2, is as small as 129.8(4)°. Opposing torsion angles in **3**$^+$ about the bonds C1–S1 and C2–S2 and related steric interactions account for this feature. In contrast, the substituents at sulfur in **2**$^+$ are both directed away from the [(PMe$_3$)$_3$Co] unit. Likely, the larger P–Co–P angles discussed above force such a close proximity of the alkyl substituents at sulfur leading in turn to large C_{sp}–C_{sp}–S angles. In addition, the position of the CoC$_2$ plane with respect to the CoP$_3$ unit is different in **2**$^+$ and **3**$^+$. In **2**$^+$ the CoC1C2 plane is nearly aligned with the Co–P2 vector rendering this bond longer than Co–P1 and Co–P3. In contrast, the CoC1C2 plane in **3**$^+$ is rather staggered rendering the Co–P2 bond perpendicular to the C1–C2 axis shorter than the other two. However, the alkyne rotates readily in solution as indicated by the observation of only one resonance in the ^{31}P NMR spectra. The ^{13}C NMR resonances of the metal bound carbon atoms at 181.8 and 182.8 ppm are in accord with a four-electron donor alkyne complex.

Addition of stoichiometric amounts of Bu$_4$NF to a solution of **3**-PF$_6$ in thf at −78 °C resulted in an immediate colour change from green to purple concomitant with ethylene evolution indicating the formation of [(triphos)Co{η^2-(S)C$_2$(SCH$_2$Ph)}], **4** (Scheme 1). The rate of this reaction is remarkable with respect to the observation that the corresponding PMe$_3$ complex **2**-PF$_6$ did not react at all with any fluoride source. The air-sensitive thioalkyne complex **4** was isolated from toluene solution and crystallized from thf/n-hexane. The result of a X-ray diffraction analysis is depicted in Fig. 3, selected interatomic distances and angles are listed in Table 1. Complex **4** crystallizes in the triclinic system with two individual molecules in the asymmetric unit. Both specimens differ only marginally.

Going from **3**$^+$ to **4**, the connectivity of the alkyne complex and the overall tetrahedral geometry at the cobalt center is remarkably retained. As observed in **3**$^+$, the CoC1C2 plane is again not aligned with one of the Co–P bonds. The Co–P2 bond, which lies approx. perpendicular to the C1–C2 vector, is of equal length in **3**$^+$ and **4**, while the other two Co–P1 and Co–P3 bonds are slightly shorter in **4**. In addition, the C1–C2 bond lengths and the mean Co–C_{sp} distances are virtually equal in **3**$^+$ and **4** {1.342(7) Å *vs.* 1.346(5) Å and 1.846(5) Å *vs.* 1.846(3) Å, respectively}. However, the thioalkyne in **4** is coordinated in a nonsymmetric fashion leading to a significantly longer Co–C1 bond compared with Co–C2. Thus, the carbon atom with the terminal sulfur atom attached is somewhat displaced from the cobalt indicating a contribution of resonance form **4B** (Fig. 3). However, the difference between C1–S1 and C2–S2 is rather insignificant. Therefore, the longer Co–C1 bond can alternatively be rationalized by charge repulsion in accord with resonance form **4A**. In addition, the position of the benzyl substituent pointing away from the cobalt alkyne moiety (torsion angle C1A–C2A–S2A–C44A 18.03°) is noticeable. Consequently, the bend-back angles C_{sp}–C_{sp}–S are larger compared with those in **3**$^+$ showing values over 140°.

Interestingly, the ^{1}H NMR resonance of the SCH$_2$ protons is found considerably low field shifted from 4.16 ppm in **3**$^+$ to 5.56 ppm in **4**. Likely, the predominant position of this CH$_2$ group in the anisotropy cone of the cobalt coordinated C–C bond as observed in the solid state structure of **4** accounts for this spectroscopic feature. The removal of an alkyl group in **3**$^+$ led only to a minor shift of the ^{31}P NMR resonance (36.4 ppm for **3**$^+$, 32.6 ppm for **4**), while the ^{13}C NMR resonances of both cobalt bound carbon atoms are detected low field shifted at 229.9 and 207.7 ppm. A correlation spectrum (qHMBC) revealed the resonance at 207.7 ppm to belong to the *C*SBn atom. Therefore, the change from a sulfide group in **3**$^+$ to a terminal sulfur atom in **4** caused a ^{13}C NMR low field shift for the directly attached carbon atom of $\Delta\delta = 48.1$ ppm. Obviously, absence of a positive charge in **4** compared to **3**$^+$, is effective predominantly at the coordinated alkyne unit but much less at the metal center itself as indicated by the negligible ^{31}P NMR shift.

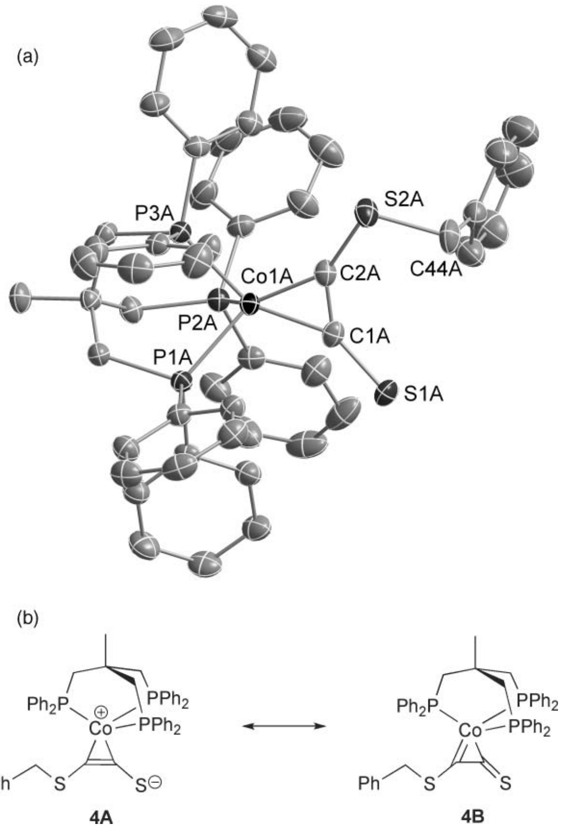

Fig. 3 Molecular structure of one specimen of **4** showing 50% probability ellipsoids and the atom labelling scheme. Hydrogen atoms are omitted for clarity.

Published on 26 November 2009. Downloaded by State University of New York at Stony Brook on 23/10/2014 19:43:42.

Table 2 Selected interatomic distances (Å) and angles (°) for 6^+ and 7^+

	6^+	7^+		6^+	7^+
Co–C1	1.821(7)	1.860(5)	Co–C2	1.832(7)	1.815(5)
C1–S1	1.714(7)	1.709(6)	C2–S2	1.693(7)	1.702(5)
Pt–S1	2.287(2)	2.358(2)	Pt–S2	2.268(2)	2.337(2)
C1–C2	1.346(10)	1.319(8)			
Co–P1	2.161(2)	2.181(2)	Pt–N1	2.071(6)	
Co–P2	2.161(2)	2.146(2)	Pt–N2	2.062(6)	
Co–P3	2.178(2)	2.147(2)	Pt–P4		2.256(2)
			Pt–P5		2.251(1)
C1–C2–S2	123.3(6)	126.5(4)			
C2–C1–S1	122.8(6)	124.4(4)			
S1–Pt–S2	89.40(6)	89.16(5)			

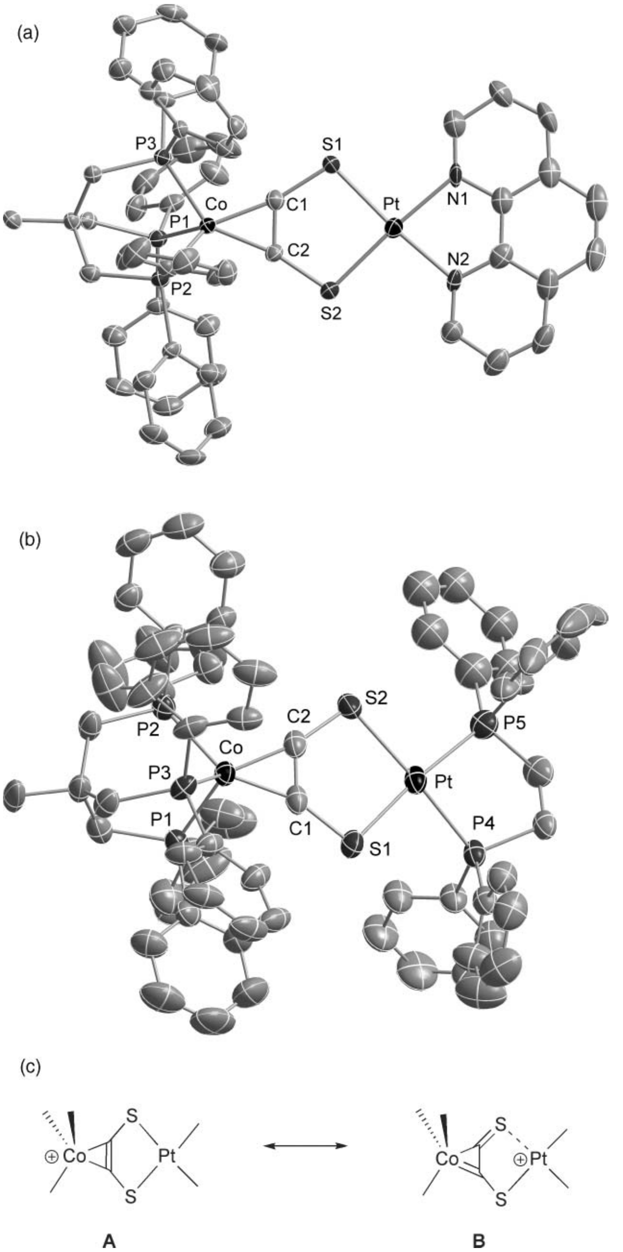

Fig. 4 Molecular structures of 6^+ (top) and 7^+ (below) showing 50% probability ellipsoids and atom labelling scheme. Hydrogen atoms and BPh_4 anions are omitted for clarity.

The half wave potential $E_{1/2}$ of **4** in thf solution was shown to be −1.44 V *vs.* Ferrocene/Ferrocenium by cyclic voltammetry. Stoichiometric reduction of **4** with C_8K in thf led to a deep green solution, which showed a single new resonance at −23 ppm in the ^{31}P NMR spectrum. A MALDI mass spectrum of the solid sample displayed an intense peak at m/z = 773 for the doubly protonated species $[(triphos)Co(C_2S_2H_2)]^+$. Therefore, we concluded that $K[(triphos)Co(\eta^2\text{-}C_2S_2)]$, K-**5**, is present in solution (Scheme 1). The complex anion 5^- turned out to be highly reactive rendering the isolation of an analytically pure sample difficult. However, we used solutions of K-**5** successfully for further coordination attempts.

The only known, structurally characterized η^2-alkyne complex of $acdt^{2-}$ displays bend-back angles of 138.3° and 143.8° leading to a long intermolecular S–S′ distance of 3.9 Å.[18] Therefore, considering the presumably large *S*,*S*′-bite angle in 5^- we felt platinum being an appropriate candidate for the formation of heterobimetallic *S*,*S*′-chelate complexes. Indeed, addition of $[PtCl_2(phen)]$ or $[PtCl_2(dppe)]$ to solutions of K-**5** in thf and the subsequent addition of $NaBPh_4$ led to a colour change to purple or red, respectively. The ^{31}P NMR spectra of the products revealed the consumption of K-**5** and a remarkable coordination shift of more than 60 ppm. The dinuclear complexes $[(triphos)Co(C_2S_2)Pt(phen)](BPh_4)$, **6**-$BPh_4$, and $[(triphos)Co(C_2S_2)Pt(dppe)](BPh_4)$, **7**-$BPh_4$, were purified by column chromatography and crystallized in moderate yields from solutions in CH_2Cl_2–n-hexane (**6**-BPh_4) or thf (**7**-BPh_4). The molecular structures of 6^+ and 7^+ determined by X-ray diffraction of **6**-BPh_4 and **7**-BPh_4 are depicted in Fig. 4 and selected interatomic distances and angles are listed in Table 2.

In both complex cations $acdt^{2-}$ adopts the η^2-*C*,*C*′-κ^2-*S*,*S*′-bridging mode with a largely planar five-membered chelate ring. The Pt centers are coordinated in a square planar fashion, while the Co alkyne complex unit is highly similar to that in 3^+ and **4**. As already observed in 3^+ and **4**, the position of the C_2S_2 plane with respect to the P3 unit at Co is rather staggered than aligned with one of the Co–P bonds. To allow for the *S*,*S*′-chelate coordination, the bend-back angles in the Co alkyne complex moiety are noticeably decreased compared with those in **4** (Table 2). However, the comparatively long intramolecular S1···S2 distances of 3.203(2) Å in 6^+ and of 3.296(2) Å in 7^+ reflect the still large *S*,*S*′- bite angle of 5^-. A detailed comparison of 6^+ and 7^+ shed light on the effect of sulfur coordination on the Co alkyne complex unit. The Pt–S bonds in the phen complex 6^+ are significantly shorter than in the dppe congener 7^+, which is consistent with an antisymbiotic effect.[29] As a result, the CoC_2S_2Pt rings in 6^+ show virtually local C_s symmetry, which does not apply to the same extent to 7^+. Therefore, the stronger electron-withdrawing effect of the [Pt(phen)] moiety leads to a higher partial charge at the alkyne complex unit, which is reflected by resonance structure **A**, while 7^+ is better represented by resonance structure **B** (Fig. 4). The effect is still visible but small at the phosphorus atoms of the triphos ligand as indicated by the ^{31}P NMR shift.

Generally, the Pt–S bond lengths in 7^+ meet those observed in thioether and dithiocarbamate complexes, and they are longer than usually observed in neutral Pt(II) dithiolene complexes with the dppe ancillary ligand (mean value 2.303 Å).[30-32] However, taking in to account the ^{31}P-^{195}Pt coupling in NMR experiments, the *trans*-effect of 5^- is even somewhat stronger compared with maleonitriledithiolate or

Published on 26 November 2009. Downloaded by State University of New York at Stony Brook on 23/10/2014 19:43:42.

Table 3 Electronic property data of **6**-BPh$_4$ and **7**-BPh$_4$

	λ/nm (ε/10^3 L mol^{-1} cm^{-1})		$E_{1/2}$ (*vs.* Fc/Fc$^+$)/V (ΔE_p/V)	
K-**5**	456[a]	593[a]	—	—
6-BPh$_4$	379 (6.5)	554 (8.8)	−1.64 (0.12)	−1.96 (0.18)
7-BPh$_4$	428 (5.9)	562 (5.2)	−1.71 (0.18)	

[a] Absorptivity uncorrected.

bis(methoxycarbonyl)ethenedithiolate. The corresponding $^1J(^{31}P-^{195}Pt)$ values are 2794 Hz for [Pt(dppe){$S_2C_2(CN)_2$}],[30] 2769 Hz for [Pt(dppe){$S_2C_2(CO_2Me)_2$}][31] and 2581 Hz for **7**$^+$. An exceptional structural feature of both, **6**$^+$ and **7**$^+$, is the folding of the CoC$_2$S$_2$ unit about the $C_{sp}\cdots C_{sp}$ axis. The angles between best calculated planes including the atoms CoC1C2 and C1C2S1S2Pt amount to 7.8(3)° in **6**$^+$ and 11.4(2)° in **7**$^+$.

Interestingly, we have not been able to isolate the related homoleptic complex [Pt(**5**)$_2$] by reaction of K-**5** with various Pt precursors like [PtCl$_2$(NCPh)$_2$]. In contrast, the related W(II) complex anion [Tp′W(CO)$_2$(acdt)]$^-$ forms trimetallic neutral complexes with all divalent group 10 metal ions (see Fig. 1). Examination of reaction mixtures with Pt^{2+} and **5**$^-$ indicated by mass and ^{31}P NMR spectroscopy the formation of the cation [(triphos)Co(C$_2$S$_2$)Pt(triphos)]$^+$. Obviously, the triphos ligand is rather labile in K-**5**. This observation can be rationalized by the high field shifted ^{31}P NMR resonance of K-**5** ($\delta_P = -23.0$ ppm), which is literally equal to the resonance of free triphosphine.

The electronic absorption spectra of heterobimetallic **6**-BPh$_4$ and **7**-BPh$_4$ display high similarity with the spectrum of monometallic K-**5** (Fig. 5). We conclude that the two high extinction absorption bands in the visible part of the spectrum are due to the cobalt alkyne moiety. This assignment is supported by the observation that both bands are blue shifted as a result of Pt coordination at the sulfur centers. Combined σ-donor and π-donor effects of sulfur to platinum stabilize the HOMOs of **5**$^-$ leading to a transition of slightly higher energy. Consistently, this hypsochromic coordination shift is more pronounced in the phen complex **6**-BPh$_4$ with the shorter Pt–S bonds (Table 3). By comparison with related tdt^{2-} complexes of Pt(II)[33] the shoulders at 700 and 680 nm for **6**$^+$ and **7**$^+$, respectively, can be assigned to a sulfur to platinum charge transfer, the intensity of which being comparatively low.

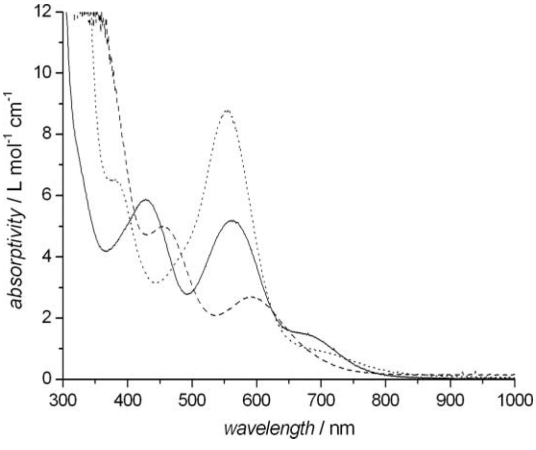

Fig. 5 Electronic absorption spectra of K-**5** (broken line), **6**-BPh$_4$ (dotted line) and **7**-BPh$_4$ (line) in thf solution, absorptivity of K-**5** is uncorrected.

Cyclic voltammetry studies revealed that both complexes can be reduced at fairly low potential (Table 3). The redox wave of **7**-BPh$_4$ shows quasi-reversible behavior with ΔE = 180 mV (Fig. 6). Stoichiometric reduction experiments with **7**-BPh$_4$ proved the chemical reversibility of the reduction by subsequent reoxidation as indicated by electronic absorption spectroscopy. Differing from **7**-BPh$_4$, the voltammogram of **6**-BPh$_4$ displays two redox processes in the potential range of interest. Very likely, the second process is due to the reduction of the phenanthroline ligand, which is expected at such a potential.[34] Interestingly, stoichiometric one-electron reduction of **6**-BPh$_4$ does not lead to a paramagnetic complex, while formation of paramagnetic **7** was proven (*vide infra*).

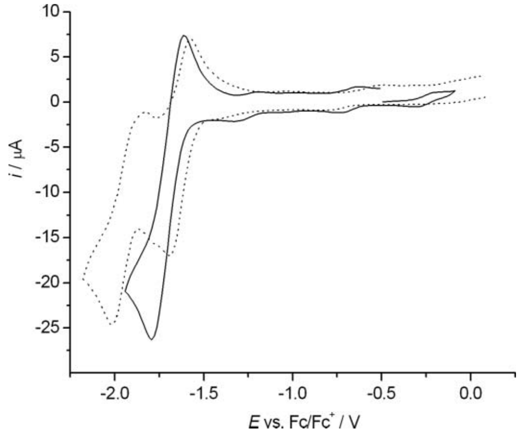

Fig. 6 Cyclic voltammograms of **6**-BPh$_4$ (dotted line) and **7**-BPh$_4$ (line) in CH$_2$Cl$_2$, scan rate 100 mV s^{-1}, **6**-BPh$_4$ measured at −78 °C.

In order to gain information on the spin density distribution and the related physical oxidation states of the metals in **7** we performed X-band EPR measurements in frozen thf solution. A sample of neutral **7** was prepared *in situ* by reduction of **7**$^+$ with Na-naphthalide in thf. The spectrum displays a rhombic **g**-tensor with intricate hyperfine splitting (Fig. 7). Due to the high number of potential hyperfine coupling partners the spectrum is very difficult to elucidate coherently. However, the signal is clearly based on a triplet structure originating from coupling to the ^{31}P atoms of

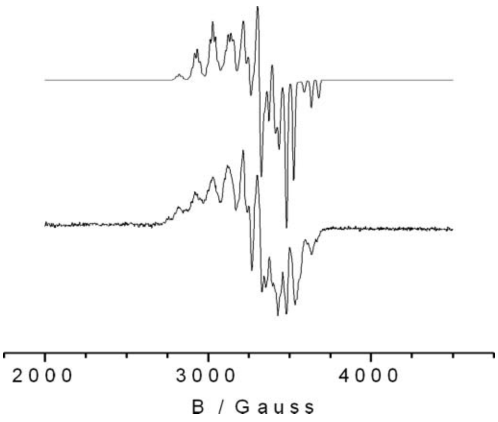

Fig. 7 X-band EPR spectrum of **7** in frozen thf solution (30 K, bottom), simulation (above).

This journal is © The Royal Society of Chemistry 2010

Published on 26 November 2009. Downloaded by State University of New York at Stony Brook on 23/10/2014 19:43:42.

dppe together with ^{195}Pt satellites. Because for ^{59}Co with $I = 7/2$ and 100% abundance a completely different pattern is anticipated, a noticeable contribution of the spin density at the Co center can be excluded. Therefore, the neutral complex **7** is preferably regarded as Pt(I) complex. The result of simulation studies revealed principle **g**-tensor component values of $g_1 = 2.22$, $g_2 = 2.03$ and $g_3 = 1.93$ and hyperfine coupling constants of $A(^{195}\text{Pt}) = 12$–30 mT and $A(^{31}\text{P}) = 4$–10 mT (see ESI† for details). The **g**-tensor anisotropy is larger compared with those in [(dppe)PtS$_2$C$_2$Ph$_2$],[35] but it is in agreement with literature data for related bis(dithiolene) complexes.[36-38] However, the hyperfine coupling to Pt is stronger compared with (Bu$_4$N)[Pt(3,5-bis-^{t}BuC$_6$H$_2$S$_2$)] displaying $A(^{195}\text{Pt})$-values about 10 mT. This can be considered as an indication of less delocalisation of the spin density in the acdt^{2-} ligand and a higher Pt contribution in the SOMO of **7**. Nevertheless, an interpretation as genuine Pt(I)-5d^9 ground state is not appropriate, because $g_1 \gg g_{2,3} > g_{el}$ and $A_1 \gg A_{2,3}$ are expected for a square planar coordination environment.[39]

Conclusion

Our investigations with the d^9 metal ion Co(I) show that alkyne complexes of the [(triphos)Co] moiety are suitable for the stabilization of acetylenedithiolate as η^2-*C*,*C*′-complexes with two formally negatively charged terminal sulfur atoms. The preparation of [(triphos)Co(acdt)]$^-$, **5**$^-$, was achieved by subsequent removal of two different *S*-protection groups in the corresponding cationic acetylenedisulfide complex **3**$^+$ by nucleophilic cleavage in the first step and a reductive procedure in the second. Several attempts with different phosphines uncovered that the procedure is very sensitive to the type of phosphine. Thus, the PMe$_3$ complex **2**-PF$_6$ does not react with fluoride-ions, while a corresponding Co(I) complex with **1** and PPh$_2$Me could not be isolated at all.

Heterobimetallic complexes with Co(I) and Pt(II) bridged by acdt^{2-} in the μ-η^2-*C*,*C*′-κ^2-*S*,*S*′-mode could be isolated with phen and dppe ancillary ligands at platinum leading to cationic complexes [(phen)Pt(**5**)]$^+$, **6**$^+$, and [(dppe)Pt(**5**)]$^+$, **7**$^+$. However, several attempts to isolate the homoleptic complex [Pt(**5**)$_2$] failed. Probably, the overall positive charge in **6**$^+$ and **7**$^+$ releases the high electron density of the metalla-acetylendithiolate ligand **5**$^-$, which is less effective in neutral complex species. In addition, a mutual destabilization of **5**$^-$ in hypothetic [Pt(**5**)$_2$] can be considered as an antisymbiotic effect.

According to cyclic voltammetry, electronic absorption and EPR spectroscopy, the visible spectra of **6**$^+$ and **7**$^+$ are dominated by the cobalt alkyne complex moiety, while the observable redox chemistry is rather platinum based. Extension of the investigations on palladium and nickel on the one hand, and on a broader variety of ancillary ligands on the other will further strengthen this perception.

Experimental

All manipulations were carried out under a dry argon atmosphere using standard Schlenk techniques. Solvents were dried by standard methods and freshly distilled prior to use. NMR spectra were recorded on Bruker Avance I 400 (400 MHz), Avance II 200 (200 MHz) and Avance III 400 (400 MHz) spectrometers. Elemental analyses were carried out on a Vario EL III CHNS-Elemental Analyzer. MALDI mass spectra were recorded on a Bruker Reflex IV spectrometer. X-band EPR spectra were recorded on a Bruker ELEXSYS E500 spectrometer equipped with a helium flow cryostat (Oxford Instruments ESR 910) and Hewlett-Packard frequency counter HP5253B. EPR simulations were performed with the W95epr program written by F. Neese (University of Bonn and MPI for Bioinorganic Chemistry, Mülheim). Me$_3$SiC$_2$H$_4$SCCSiMe$_3$,[40] [(PMe$_3$)$_3$Co(Br)],[41] [(triphos)Co(Br)],[42] [PtCl$_2$(phen)][43] and [PtCl$_2$(dppe)] were prepared according to literature methods.

X-Ray crystallographic investigations and crystal data

Single crystals suitable for X-ray diffraction were coated in paratone oil and mounted on a glass fiber. The intensity data of the complexes was collected on a Bruker AXS Apex system equipped with a rotating anode. The data was measured using either graphite monochromated Mo-Kα radiation (**2**-PF$_6$, **3**-PF$_6$, **4**, **7**-BPh$_4$) or goebel-mirror monochromated Cu-Kα radiation (**6**-BPh$_4$). Data collection, cell refinement, data reduction and integration as well as absorption correction were performed with the Bruker AXS program packages SMART, SAINT and SADABS. Crystal and space group symmetries were determined using the XPREP program. All crystal structures were solved with SHELXS[44] by direct methods and were refined by full-matrix least-square techniques against F_o^2 with SHELXL.[45] All non-hydrogen atoms were refined anisotropically. The hydrogen atoms were included at calculated positions. The details of the structure analyses are listed in Table 4.

Preparations

1-Trimethylsilyl-7-phenyl-3,6-dithiahept-4-ine (1). A solution of Me$_3$SiC$_2$H$_4$SCCSiMe$_3$ (8.53 g, 37.00 mmol) in thf (100 mL) was cooled to −78 °C. Methyllithium·lithium bromide (2.2 M solution in Et$_2$O, 16.8 mL, 37.00 mmol) was added and the resulting yellow solution was stirred for half an hour at this temperature. Subsequently, the mixture was slowly warmed to 0 °C and stirred for two hours at this temperature. After again being cooled to −78 °C, sulfur (1.18 g, 37.00 mmol) was added. The mixture was stirred for 20 min at −78 °C and then warmed to room temperature. To the resulting clear solution was added benzyl bromide (4.4 mL, 37.00 mmol) at 0 °C. After stirring overnight at ambient temperature, the solvents were evaporated and the residue purified by column chromatography on SiO$_2$ (*n*–hexane–toluene 5 : 1). **1** was obtained as a yellow oil (9.97 g, 96%). Found: C, 60.64; H, 7.14; S, 22.67. C$_{14}$H$_{20}$S$_2$Si·0.05 C$_7$H$_8$ requires C, 60.45; H, 7.21; S 22.49%; δ_H(400 MHz; CDCl$_3$) 7.36–7.30 (5 H, m, Ph-*H*), 3.92 (2 H, s, C*H*$_2$Ph), 2.70 (2 H, m, C*H*$_2$CH$_2$SiMe$_3$), 0.93 (2 H, m, CH$_2$C*H*$_2$SiMe$_3$), 0.05 (9 H, s, Si(C*H*$_3$)$_3$); δ_C(101 MHz; CDCl$_3$) 136.6, 129.1, 128.4, 127.6 (Ph-*C*), 88.5 (Me$_3$SiC$_2$H$_4$S*C*≡C), 86.4 (C≡*C*SBn), 41.5 (*C*H$_2$Ph), 33.0 (*C*H$_2$CH$_2$SiMe$_3$), 17.1 (CH$_2$*C*H$_2$SiMe$_3$), −1.8 (Si(*C*H$_3$)$_3$).

[(PMe$_3$)$_3$Co(1)](PF$_6$) (2-PF$_6$). A solution of [(PMe$_3$)$_3$Co(Br)] (300 mg, 0.82 mmol) in CH$_3$CN (20 mL) was treated with **1** (460 mg, 1.64 mmol). The color of the solution turned green immediately. After 30 min, KPF$_6$ (165 mg, 0.90 mmol) was added and the solution stirred overnight. The solvent was removed *in vacuo* and the residue dissolved in CH$_2$Cl$_2$ (20 mL). After

Published on 26 November 2009. Downloaded by State University of New York at Stony Brook on 23/10/2014 19:43:42.

Table 4 Crystal data, data collection and structure refinement for complexes **2**-PF_6, **3**-PF_6, **4**, **6**-BPh_4 and **7**-BPh_4

Compound	**2**-PF_6	**3**-PF_6	**4**	**6**-BPh_4	**7**-BPh_4
Formula	$C_{23}H_{47}CoF_6P_4S_2Si$	$C_{55}H_{59}CoF_6P_4S_2Si\cdot 2CH_3OH$	$C_{100}H_{92}Co_2P_6S_4\cdot 1.5thf$	$C_{79}H_{67}BCoN_2P_3PtS_2$	$C_{93}H_{83}BCoP_5PtS_2\cdot 0.5thf$
Formula weight	712.63	1109.09	1725.76	1466.21	1684.48
Crystal system	Monoclinic	Triclinic	Triclinic	Triclinic	Monoclinic
Space group	$P2_1/c$	$P\bar{1}$	$P\bar{1}$	$P\bar{1}$	$P2_1/n$
a/Å	11.7241(7)	14.5606(14)	14.067(2)	11.1143(6)	12.3583(3)
b/Å	23.9821(14)	15.0042(15)	15.000(2)	17.6581(12)	19.5334(5)
c/Å	12.5138(8)	15.4084(15)	25.050(2)	18.2065(11)	34.3595(10)
α (°)	90	65.400(2)	79.982(3)	64.204(4)	90
β (°)	101.5140(10)	78.203(2)	78.203(2)	89.668(4)	94.1190(10)
γ (°)	90	67.958(2)	77.636(3)	89.378(5)	90
V/Å^3	3447.7	2832.4(5)	4615.6(10)	3216.9(3)	8272.9(4)
Z	4	2	2	2	4
T/K	153	153	153	153	153
$2\Theta_{max}$ (°)	55.76	47.00	55.76	145.18	49.70
μ/mm^{-1}	0.885	0.572	0.604	7.704	2.086
Refls collected	18610	20087	46827	19176	65527
Refls unique (R_{int})	8208 (0.0305)	8393 (0.0560)	21988 (0.0414)	10952 (0.1120)	14303 (0.0467)
Parameters/restraints	346/0	666/0	1045/0	803/0	949/9
R_1 [$I > 2\sigma(I)$]	0.0370	0.0700	0.0606	0.0688	0.0467
wR_2 (all data)	0.0953	0.1686	0.1689	0.1737	0.1251
Resid. density/e Å^{-3}	0.582/–0.563	1.584/–0.858	1.493/–0.694	3.316/–2.008	2.359/–1.338

filtration, pure **2**-PF_6 was obtained as a green solid by crystallization from CH_2Cl_2–n-hexane (460 mg, 79%). δ_H(400 MHz; $CDCl_3$) 7.33 (5 H, m, Ph-*H*), 4.29 (2 H, s, C*H*$_2$Ph), 3.12 (2 H, m, C*H*$_2$CH$_2$SiMe$_3$), 1.49 (27 H, s, P(C*H*$_3$)$_3$), 0.99 (2 H, m, CH$_2$C*H*$_2$SiMe$_3$), 0.04 (9 H, s, Si(C*H*$_3$)$_3$); δ_C(101 MHz; CD_2Cl_2) 172.6, 170.6 (*C*≡C), 135.3, 129.0, 128.9, 128.0 (Ph-*C*), 44.1 (*C*H$_2$Ph), 36.0 (*C*H$_2$CH$_2$SiMe$_3$), 19.7 (P(*C*H$_3$)$_3$), 17.3 (CH$_2$*C*H$_2$SiMe$_3$), –2.0 (Si(*C*H$_3$)$_3$); δ_P(162 MHz; $CDCl_3$) 9.3 (*P*Me$_3$), –144.2 (*P*F$_6$).

[(triphos)Co(1)](PF$_6$) (3-PF$_6$). The compound was prepared as described for **2**-PF_6 using [(triphos)Co(Br)] (800 mg, 1.05 mmol) and **1** (590 mg, 2.11 mmol). **3**-PF_6 was obtained as a green solid after column chromatography on SiO_2 using CH_2Cl_2–MeOH (10 : 1) as eluent (1.01 g, 87%). δ_H(200 MHz; $CDCl_3$) 7.35–6.97 (35 H, m, Ph-*H*), 4.16 (2 H, s, C*H*$_2$Ph), 3.10 (2 H, m, C*H*$_2$CH$_2$SiMe$_3$), 2.44 (6 H, s, triphos-C*H*$_2$), 1.72 (3 H, s, triphos-C*H*$_3$), 0.97 (2 H, m, CH$_2$C*H*$_2$SiMe$_3$), –0.12 (9 H, s, Si(C*H*$_3$)$_3$); δ_C(101 MHz; $CDCl_3$) 182.8, 181.8 (*C*≡C), 135.5, 134.3, 131.5, 130.0, 128.8, 128.7, 128.5, 127.8 (Ph-*C*), 43.2 (*C*H$_2$Ph), 38.0 (triphos-*C*$_{quart.}$), 36.5 (triphos-*C*H$_3$), 35.3 (*C*H$_2$CH$_2$SiMe$_3$), 33.5 (triphos-*C*H$_2$), 17.9 (CH$_2$*C*H$_2$SiMe$_3$), –1.8 (Si(*C*H$_3$)$_3$); δ_P(81 MHz; $CDCl_3$) 36.4 (triphos-*P*), –143.9 (*P*F$_6$); MS (MALDI) *m*/*z* 963 (M$^+$).

[(triphos)Co{η^2-(S)C$_2$(SCH$_2$Ph)}] (4). At –78 °C Bu$_4$NF (110 mg, 0.39 mmol) was added to a solution of **3**-PF_6 (400 mg, 0.36 mmol) in thf (30 mL) leading to an intensely purple solution. The mixture was stirred for 12 h at room temperature. The solvent was evaporated and the residue redissolved in toluene. The mixture was filtered to remove Bu$_4$NPF$_6$. Crystallization from thf/n-hexane yielded dark purple crystals (230 mg, 74%). Found: C, 69.48; H, 5.59; S, 7.04. $C_{50}H_{46}CoP_3S_2\cdot thf$ requires C, 69.37; H, 5.82; S 6.86%; δ_H(400 MHz; C_6D_6) 7.58, 7.10, 6.99 (5 H, m, CH$_2$Ph), 7.39, 6.81, 6.80 (30 H, m, triphos-Ph), 5.56 (2 H, s, C*H*$_2$Ph), 2.04 (6 H, s, triphos-C*H*$_2$), 1.13 (3 H, s, triphos-C*H*$_3$); δ_C(101 MHz; d^8-thf) 229.9 (S*C*≡CSBn), 207.7 (SC≡*C*SBn), 142.2, 139.5, 133.0, 130.7, 129.0, 128.8, 128.5, 128.2 (Ph-*C*), 35.2 (*C*H$_2$Ph), 38.0 (triphos-*C*$_{quart.}$), 37.2 (triphos-*C*H$_3$), 32.8 (triphos-*C*H$_2$); δ_P(162 MHz; $CDCl_3$) 32.6 (triphos-*P*); MS (MALDI) *m*/*z* 862 (M$^+$).

K[(triphos)Co(η^2-C$_2$S$_2$)] (K-5). At –78 °C C$_8$K (56 mg, 0.42 mmol) was added to a solution of **4** (200 mg, 0.23 mmol) in thf (15 mL) leading to an intensely green solution. The mixture was stirred for 2 h at room temperature. This solution was used in the following experiments without further purification. δ_P(162 MHz; d^8-thf) –23.0 (triphos-*P*); MS (MALDI) *m*/*z* 773 (M$^-$ + 2H$^+$).

[(triphos)Co(μ-η^2-*C*,*C*′-κ^2-*S*,*S*′-C$_2$S$_2$)Pt(phen)](BPh$_4$) (6-BPh$_4$). [PtCl$_2$(phen)] (45 mg, 0.10 mmol) was added to a solution of K-**5** (75 mg, 0.09 mmol) in thf (20 mL). After subsequent addition of NaBPh$_4$ (120 mg, 0.35 mmol), the solution was stirred for 18 h. The solvent was removed and the crude product purified by column chromatography on SiO_2 using CH_2Cl_2–n-hexane (10 : 1) as eluent. After crystallization (CH_2Cl_2–n-hexane) the compound was isolated as a purple solid (48 mg, 32%). Found: C, 64.31; H, 4.58; N, 1.88; S, 4.10. $C_{79}H_{67}BCoN_2P_3PtS_2$ requires C, 64.71; H, 4.61; N 1.91; S 4.37%; δ_H(400 MHz; CD_2Cl_2) 9.52, 8.57, 7.93, 7.82 (8 H, m, phen-*H*), 7.34 (20 H, m, BPh$_4$), 7.13, 7.03, 6.88 (30 H, m, triphos-Ph), 2.35 (6 H, s, triphos-C*H*$_2$), 1.66 (3 H, s, triphos-C*H*$_3$); δ_C(101 MHz; CD_2Cl_2) 230.9 (*C*≡C), 164.4 (B–C$_i$), 151.7, 146.8, 139.0, 136.4, 135.5, 131.9, 131.7, 130.0, 129.3, 129.1, 128.7, 128.3, 126.0 (Ph-*C*), 38.3 (triphos-*C*$_{quart.}$), 37.3 (triphos-*C*H$_3$), 33.4 (triphos-*C*H$_2$); δ_P(162 MHz; CD_2Cl_2) 43.4 (triphos-*P*); MS (MALDI) *m*/*z* 1146 (M$^+$).

[(triphos)Co(μ-η^2-*C*,*C*′-κ^2-*S*,*S*′-C$_2$S$_2$)Pt(dppe)](BPh$_4$) (7-BPh$_4$). The compound was prepared as described for **6**-BPh$_4$ using K-**5** (74 mg, 0.09 mmol), [PtCl$_2$(dppe)] (63 mg, 0.09 mmol) and NaBPh$_4$ (117 mg, 0.34 mmol). **7**-BPh$_4$ was obtained as a red solid after column chromatography on SiO_2 using CH_2Cl_2/*n*–hexane (5 : 1) as eluent (91 mg, 63%). Found: C, 63.79; H, 4.96; S, 3.45. $C_{93}H_{83}BCoP_5PtS_2\cdot CH_2Cl_2$ requires C, 63.81; H, 4.84; S 3.62%; δ_H(400 MHz; CD_2Cl_2) 7.89–6.83 (70 H, m, Ph-*H*), 2.38 (4 H, m, dppe), 2.28 (6 H, s, triphos-C*H*$_2$), 1.59 (3 H, s, triphos-C*H*$_3$);

This journal is © The Royal Society of Chemistry 2010

Published on 26 November 2009. Downloaded by State University of New York at Stony Brook on 23/10/2014 19:43:42.

δ_C(101 MHz; $CDCl_3$) 242.1 ($C{\equiv}C$), 164.2 (B–C_i), 141.2, 136.3, 134.9, 133.5, 131.8, 131.4, 129.0, 128.7, 127.9, 127.1, 125.4 (Ph-C), 37.8 (triphos-$C_{quart.}$), 37.2 (triphos-CH_3), 33.3 (triphos-CH_2), 27.5 (dd, $^1J_{CP}$ = 38.7 Hz, $^2J_{CP}$ = 11.9 Hz, dppe); δ_P(162 MHz; CD_2Cl_2) 45.3 ($^1J_{PPt}$ = 2581 Hz, dppe-P), 42.3 (triphos–P); MS (MALDI) m/z 1365 (M^+).

Acknowledgements

We are grateful to the Deutsche Forschungsgemeinschaft and the Fonds of Chemical Industry (VCI) for an award for M.J.M. We thank Dr. E. Bill (MPI Mülheim) for the EPR measurement. W.W.S. thanks Prof. F. E. Hahn for generous support.

Notes and references

1 O. Kahn, *Acc. Chem. Res.*, 2000, **33**, 647–657.
2 J. S. Miller and J. L. Manson, *Acc. Chem. Res.*, 2001, **34**, 563–570.
3 L. M. C. Beltran and J. R. Long, *Acc. Chem. Res.*, 2005, **38**, 325–334.
4 T. Glaser, M. Heidemeier, T. Weyhermüller, R.-D. Hoffmann, H. Rupp and P. Müller, *Angew. Chem.*, 2006, **118**, 6179–6183; T. Glaser, M. Heidemeier, T. Weyhermüller, R.-D. Hoffmann, H. Rupp and P. Müller, *Angew. Chem., Int. Ed.*, 2006, **45**, 6033–6037.
5 R. T. F. Jukes, V. Adamo, F. Hartl, P. Belser and L. De Cola, *Coord. Chem. Rev.*, 2005, **249**, 1327–1335.
6 J. L. Dempsey, A. J. Esswein, D. R. Manke, J. Rosenthal, J. D. Soper and D. G. Nocera, *Inorg. Chem.*, 2005, **44**, 6879–6892.
7 S. Rau, B. Schaefer, D. Gleich, E. Anders, M. Rudolph, M. Friedrich, H. Goerls, W. Henry and J. G. Vos, *Angew. Chem.*, 2006, **118**, 6361–6364; S. Rau, B. Schaefer, D. Gleich, E. Anders, M. Rudolph, M. Friedrich, H. Goerls, W. Henry and J. G. Vos, *Angew. Chem., Int. Ed.*, 2006, **45**, 6215–6218.
8 E. Cerrada, M. Laguna and N. Lardies, *Eur. J. Inorg. Chem.*, 2009, 137–146.
9 W. Weigand, *Z. Naturforsch.*, 1991, **46b**, 1333–1337.
10 W. Weigand, M. Weishäupl and C. Robl, *Z. Naturforsch.*, 1996, **51b**, 501–505.
11 H. Sugiyama, Y. Hayashi, H. Kawaguchi and K. Tatsumi, *Inorg. Chem.*, 1998, **37**, 6773–6779.
12 Y. Sunada, Y. Hayashi, H. Kawaguchi and K. Tatsumi, *Inorg. Chem.*, 2001, **40**, 7072–7078.
13 I. Ara, E. Delgado, J. Fornies, E. Hernandes, E. Lalinde, N. Mansilla and M. T. Moreno, *J. Chem. Soc., Dalton Trans.*, 1998, 3199–3208.
14 R.-J. Wang, L.-C. Song, H.-G. Wang, Z.-X. Wang and J.-T. Wang, *Huaxue Xuebao*, 1989, **47**, 16.
15 E. Delgado, M. I. Alcalde, B. Donnadieu, E. Hernandez and J. Sanchez-Nieves, *Acta Crystallogr., Sect. E: Struct. Rep. Online*, 2003, **59**, m207–m209.
16 W. W. Seidel, M. Schaffrath and T. Pape, *Angew. Chem.*, 2005, **117**, 7976–7979; W. W. Seidel, M. Schaffrath and T. Pape, *Angew. Chem., Int. Ed.*, 2005, **44**, 7798–7800.
17 W. W. Seidel, M. Schaffrath and T. Pape, *Chem. Commun.*, 2006, 3999–4000.
18 W. W. Seidel, M. J. Meel, U. Radius, M. Schaffrath and T. Pape, *Inorg. Chem.*, 2007, **46**, 9616–9629.
19 F. Diehl, H. Meyer, A. Schweig, B. A. Hess Jr. and J. Fabian, *J. Am. Chem. Soc.*, 1989, **111**, 7651–7653.
20 A. Timoshkin and G. Frenking, *J. Chem. Phys.*, 2000, **113**, 8430–8433.
21 D. Vijay and G. N. Sastry, *THEOCHEM*, 2005, **732**, 71–78.
22 W. W. Seidel, M. D. Ibarra Arias, M. Schaffrath, M. Jahnke, A. Hepp and T. Pape, *Inorg. Chem.*, 2006, **45**, 4791–4800.
23 K. P. C. Vollhardt, *Acc. Chem. Res.*, 1977, **10**, 1–8.
24 V. Gandon, N. Agenet, K. P. C. Vollhardt, M. Malacria and C. Aubert, *J. Am. Chem. Soc.*, 2006, **128**, 8509–8520.
25 T. H. Staeb, J. Chavez, R. Gleiter and B. Nuber, *Eur. J. Inorg. Chem.*, 2005, 4090–4093.
26 B. Capelle, M. Dartiguenave, Y. Dartiguenave and A. L. Beauchamp, *J. Am. Chem. Soc.*, 1983, **105**, 4662–4670.
27 A. Bouayad, M. Dartiguenave, M.-J. Menu, Y. Dartiguenave, F. Belanger-Gariepy and A. L. Beauchamp, *Organometallics*, 1989, **8**, 629–637.
28 R. Rupp, G. Huttner, H. Lang, K. Heinze, M. Buchner and E. R. Hovestreydt, *Eur. J. Inorg. Chem.*, 2000, 1953–1959.
29 R. G. Pearson, *Inorg. Chem.*, 1973, **12**, 712–713.
30 R. Vicente, J. Ribas, X. Solans, M. Font-Altaba, A. Mari, P. de Loth and P. Cassoux, *Inorg. Chim. Acta*, 1987, **132**, 229–236.
31 J. M. Bevilacqua, J. A. Zuleta and R. Eisenberg, *Inorg. Chem.*, 1994, **33**, 258–266.
32 S. Ford, M. R. Lewtas, C. P. Morley and M. Di Vaira, *Eur. J. Inorg. Chem.*, 2000, 933–938.
33 W. Paw, W. B. Connick and R. Eisenberg, *Inorg. Chem.*, 1998, **37**, 3919–3926.
34 A. Klein, W. Kaim, E. Waldhoer and H.-D. Hausen, *J. Chem. Soc., Perkin Trans. 2*, 1995, 2121–2126.
35 G. A. Bowmaker, P. W. D. Boyd and G. K. Campbell, *Inorg. Chem.*, 1983, **22**, 1208–1213.
36 A. Davison, N. Edelstein, R. H. Holm and A. H. Maki, *Inorg. Chem.*, 1964, **3**, 814–823.
37 J. A. Tang, E. Kogut, D. Norton, A. J. Lough, B. R. McGarvey, U. Fekl and R. W. Schurko, *J. Phys. Chem. B*, 2009, **113**, 3298–3313.
38 K. Ray, T. Weyhermüller, F. Neese and K. Wieghardt, *Inorg. Chem.*, 2005, **44**, 5345–5360.
39 P. S. Braterman, J.-I. Song, F. M. Wimmer, S. Wimmer, W. Kaim, A. Klein and R. D. Peacock, *Inorg. Chem.*, 1992, **31**, 5084–5088.
40 W. W. Seidel, M. J. Meel, M. Schaffrath and T. Pape, *Eur. J. Org. Chem.*, 2007, 3526–3532.
41 H. F. Klein and H. H. Karsch, *Inorg. Chem.*, 1975, **14**, 473–477.
42 L. Sacconi and S. Midollini, *J. Chem. Soc., Dalton Trans.*, 1972, 1213–1216.
43 A. R. Sanger, *J. Chem. Soc., Dalton Trans.*, 1977, 1971–1976.
44 G. M. Sheldrick, *SHELXS-97: Program for solution of crystal structures*, Universität Göttingen, Germany, 1997.
45 G. M. Sheldrick, *SHELXL-97: Program for refinement of crystal structures*, Universität Göttingen, Germany, 1997.